

Spatial coherence radar applied for tilted surface profilometry

Mark Gokhler

Ben Gurion University of the Negev
Department of Electrical and Computer
Engineering
P.O. Box 653
Beer-Sheva 84105, Israel

Zhihui Duan

The University of Electro-Communications
1-5-1 Chofugaoka, Chofu
Tokyo 182-8585, Japan

Joseph Rosen, MEMBER SPIE

Ben Gurion University of the Negev
Department of Electrical and Computer
Engineering
P.O. Box 653
Beer-Sheva 84105, Israel
E-mail: rosen@ee.bgu.ac.il

Mitsuo Takeda, FELLOW SPIE

The University of Electro-Communications
1-5-1 Chofugaoka, Chofu
Tokyo 182-8585, Japan

1 Introduction

Optical coherence profilometry^{1,2} is a noninvasive sensing method that provides profile information with high resolution and high sensitivity. Most of the systems of this kind operate by the principle of temporal coherence.³ Recently, several attempts to explore the principle of longitudinal spatial coherence for coherence profilometry have been made.⁴⁻⁶ The coherence between two points along the propagation axis can be determined purely by the extent of a quasimonochromatic incoherent planar source according to a particular interpretation of the Van Cittert-Zernike theorem. Rosen and Takeda⁵ have shown that the effect could be useful for measuring three-dimensional profiles of rough surfaces. Two features are characteristic of this new technique. First, a quasimonochromatic light illuminates the system, and that gives an inherent immunity from effects of dispersion. Second, the surface profile is measured without shifting the sample or the reference mirror. This last feature can save mechanical movements and may enable the measurement of surfaces that cannot move relative to the reference mirror.

In this study we explore more deeply the recently invented method of spatial coherence profilometry without mechanical movements.^{5,6} The heart of the method is the control on the shape of the spatial degree of coherence. The surface profile is measured by means of nonmechanically shifting the spatial degree of coherence gradually in its space of existence while keeping the optical path difference between the interferometer's measured surface and a reference plane constant. Appearance of high interference visibility on the detector is an indication that the optical path

Abstract. A new method of spatial coherence profilometry is demonstrated. The surface profile is measured by shifting the spatial degree of coherence gradually in its own space of existence, and modulating its phase angle. In each point of the sample we analyze the change of light intensity versus the phase of a Fresnel zone pattern used as the intensity distribution of an incoherent quasimonochromatic source. The tilt of the surface is measured by gradually shifting the Fresnel zone plate on its transverse plane. This shift of the light source rotates the spatial degree of coherence around the coordinate origin until the condition of maximum interference visibility is fulfilled. The method works without any mechanical movement and a quasimonochromatic light illuminates the interferometric system. Experimental demonstration of the new method is presented. © 2003 Society of Photo-Optical Instrumentation Engineers. [DOI: 10.1117/1.1542893]

Subject terms: coherence; tomography; interferometry; surfaces.

Paper 020144 received Apr. 15, 2002; revised manuscript received Sep. 5, 2002; accepted for publication Sep. 5, 2002.

difference is equal to the amount of the shift of the spatial degree of coherence. A key element in this scheme is an electrically addressed spatial light modulator (SLM) that can spatially modulate the intensity distribution of the light. Using SLM, one can get complete control on the shape and the phase of the degree of coherence in the system without moving any component in the interferometer. There are two new elements in this study compared to Refs. 5 and 6; first the transverse, additionally to the axial, movement of the degree of coherence is demonstrated. This additional feature enables us to measure not just the elevation of a surface but also its angle of tilt relative to the reference plane. Second, the phase of the degree of coherence is modulated. This additional feature enables us to measure altitudes of small surfaces, smaller than the size of a single interference fringe.

2 Description of Spatial Coherence Profilometer

Since the theory of operation of the spatial coherence profilometer has already been reported in detail,^{5,6} it is only briefly reviewed here. A schematic illustration of the profilometer is shown in Fig. 1. A Fresnel zone pattern (FZP) is imaged by lens L_0 on a rotated diffuser, thus creating a dynamic incoherent light source. The FZP is displayed on an electrical-addressed SLM and illuminated by a laser. Light from this quasimonochromatic incoherent source propagates through lens L_1 and is split into two beams by a beamsplitter. One beam is reflected from the tested surface S and the other is reflected from the reference mirror R . The two reflected beams are combined and recorded by a CCD camera after passing through lens L_2 . Lens L_2 images the

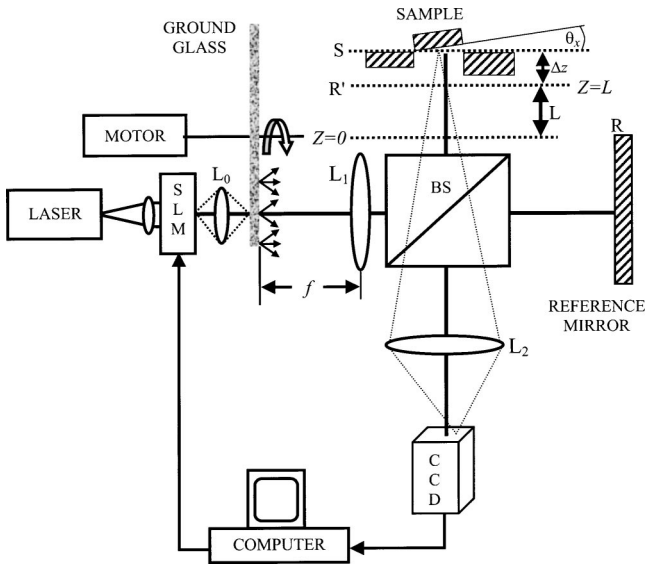


Fig. 1 Optical system for measuring surface profiles using the spatial coherence effect.

sample onto the CCD detection plane. In general we assume that the tested surface is tilted relative to the transverse plane by small angles, θ_x in the (x, z) plane and θ_y (y, z) plane. The reference mirror is assumed to be orthogonal to the optical axis, and therefore the angles (θ_x, θ_y) are also the angle differences between the sample and the virtual image of the reference mirror R' , which serves as an effective reference plane.

The point source, with a complex amplitude $u_s(x_s, y_s)$ at some point (x_s, y_s) , creates a field distribution behind the lens L_1

$$u(x, y, z) = \frac{u_s(x_s, y_s)}{j\lambda f} \exp \left[j \frac{2\pi(z+2f)}{\lambda} - j \frac{2\pi}{\lambda f} (x_s x + y_s y) - j \frac{\pi z}{\lambda f^2} (x_s^2 + y_s^2) \right], \quad (1)$$

where λ is the light wavelength, f is the focal length of lens L_1 and (x, y, z) are the coordinates behind the lens L_1 with their origin at the rear focal point. The reference R and sample mirrors S are located at distances $z=L$ and $z=L + \Delta z$, respectively, from the rear focal point. The interference fringes generated on the CCD image sensor are the result of combining the images of the two optical field distributions from the reference and the sample mirrors. Note that the beam reflected from the reference mirror travels a distance $2\Delta z$ less than the beam reflected from the S mirror. When the object surface S is tilted by a small angle (θ_x, θ_y) relative to the transverse plane, the direction of the

reflected beam deviates by an angle $(2\theta_x, 2\theta_y)$ from its original direction. This introduction of angular deviation is equivalent to giving lateral displacement $(\Delta x, \Delta y) = [f \tan(2\theta_x), f \tan(2\theta_y)]$ to the point source. Since each point source is completely incoherent to any other points on the source, the overall intensity on the image sensor contributed from all the source points is a sum of fringe intensities obtained from each point source:

$$I(x, y, L) = \iint \left| \frac{u(x_s, y_s)}{j\lambda f} \exp \left[j \frac{2\pi(L+2f)}{\lambda} - j \frac{2\pi}{\lambda f} \times (x_s x + y_s y) - j \frac{\pi L}{\lambda f^2} (x_s^2 + y_s^2) \right] + \frac{u(x_s, y_s)}{j\lambda f} \exp \left\{ j \frac{2\pi(L+2\Delta z+2f)}{\lambda} - j \frac{2\pi}{\lambda f} [(x_s - \Delta x)x + (y_s - \Delta y)y] - j \frac{\pi(L+2\Delta z)}{\lambda f^2} [(x_s - \Delta x)^2 + (y_s - \Delta y)^2] \right\} \right|^2 \times dx_s dy_s. \quad (2)$$

Note that lens L_2 images the interference distribution of two fields, one from plane R' and the other from plane S , onto the CCD plane. Therefore, regardless of the focal length of lens L_2 , Eq. (2) also describes the observed intensity on the CCD plane. Corresponding to Eq. (2), the intensity distribution on the interference plane is given by

$$I(x, y, L) = A \left\{ 1 + |\mu(\Delta x, \Delta y, 2\Delta z)| \times \cos \left[\frac{2\pi}{\lambda f} (x\Delta x + y\Delta y) - \frac{4\pi\Delta z}{\lambda} + \phi(\Delta x, \Delta y, 2\Delta z) + \frac{\pi(L+2\Delta z)}{\lambda f^2} \times (\Delta x^2 + \Delta y^2) \right] \right\}, \quad (3)$$

where

$$A = (2/\lambda^2 f^2) \iint I_s(x_s, y_s) dx_s dy_s,$$

and the function

$$\mu(\Delta x, \Delta y, 2\Delta z) = |\mu(\Delta x, \Delta y, 2\Delta z)| \exp[j\phi(\Delta x, \Delta y, 2\Delta z)]$$

is the 3-D complex degree of coherence given by⁷

$$\mu(\Delta x, \Delta y, 2\Delta z) = \frac{\iint I_s(x_s, y_s) \exp \left[j \frac{2\pi\Delta z}{\lambda f^2} (x_s^2 + y_s^2) - j \frac{2\pi(L+2\Delta z)}{\lambda f^2} (x_s \Delta x + y_s \Delta y) \right] dx_s dy_s}{\iint I_s(x_s, y_s) dx_s dy_s}. \quad (4)$$

Equation (4) is no other than the manifestation of the Van Cittert-Zernike theorem, arguing that the 3-D complex degree of coherence is determined by the intensity distribution of a quasimonochromatic incoherent source.

To probe the surface profile by only changing the spatial coherence in the system, it has been suggested in Ref. 5 to sculpt the degree of coherence in a shape of three symmetric sharp peaks, whereas one of the noncentral peaks is actually used as the probe. Because of the Fourier transform relation [as manifested by the Van Cittert-Zernike theorem in Eq. (4)] between the source intensity function and the degree of coherence, the desired three peak shape of the degree of coherence is obtained by a source intensity distribution of a transversely shifted FZP. FZP is a binary approximation of the following cosine grating

$$I_s(x_s, y_s) \propto 1 + \cos\{\pi \gamma_n [(x_s - \xi_k)^2 + (y_s - \eta_l)^2] + \beta_m\} \\ (x_s^2 + y_s^2)^{1/2} \leq R, \quad (5)$$

where R is the maximal radius of the source γ_n , (ξ_k, η_l) , and β_m are the parameters that control the longitudinal and the transverse movements and the phase of the degree of coherence, respectively. The transverse shifts given by (ξ_k, η_l) are aimed to detect tilted surfaces as shown in the following. Substituting Eq. (5) into Eq. (4) yields the following complex degree of coherence,

$$\mu(\Delta x, \Delta y, 2\Delta z) \\ \text{sinc}\left(\frac{\Delta z R^2}{2\lambda f^2}\right) \frac{J_1\left[\frac{L+2\Delta z}{\lambda f^2} 2\pi R(\Delta x^2 + \Delta y^2)^{1/2}\right]}{\frac{L+2\Delta z}{\lambda f^2} R(\Delta x^2 + \Delta y^2)^{1/2}} \\ * \left[2\delta(\Delta z) + \exp(j\beta_m) \delta\left(\Delta z + \frac{\gamma_n \lambda f^2}{2}, \Delta x \right. \right. \\ \left. \left. + \frac{\gamma_n \lambda f^2 \xi_k}{L+2\Delta z}, \Delta y + \frac{\gamma_n \lambda f^2 \eta_l}{L+2\Delta z}\right) \right. \\ \left. + \exp(-j\beta_m) \delta\left(\Delta z - \frac{\gamma_n \lambda f^2}{2}, \Delta x - \frac{\gamma_n \lambda f^2 \xi_k}{L+2\Delta z}, \Delta y \right. \right. \\ \left. \left. - \frac{\gamma_n \lambda f^2 \eta_l}{L+2\Delta z}\right) \right], \quad (6)$$

where the asterisk means convolution, δ is the Dirac delta function, J_1 is the first order, first kind, Bessel function, and $\text{sinc}(x) = \sin(\pi x)/\pi x$. In these expressions the parameters γ_n and (ξ_k, η_l) determine the location of the +1 and -1 coherence orders (equivalent to the diffraction orders) in the space $(\Delta x, \Delta y, \Delta z)$, and the parameter β_m is the phase of the ± 1 orders. For every value of γ_n and (ξ_k, η_l) , one can introduce m different values of β_m equally distributed in the range $[0, 2\pi p]$, where p is the number of periods. As the number of periods increases, the surface position is measured with less uncertainty. According to Eq. (3) the phase change of $\mu(\Delta x, \Delta y, \Delta z)$ moves the fringes in the (x, y, L) plane. Thus, if a single point on the (x, y, L) plane is probed, the detected intensity is periodically modulated

along the variable m in the same visibility value equal to $|\mu(\Delta x, \Delta y, \Delta z)|$. This method of coherence profilometry is applied herein, enabling us to measure surfaces with an area smaller than the width of a single spatial fringe. At each spatial point we measure the modulation depth of each periodic intensity signal of p periods. The aim of this measurement is to find the maximum value of the modulation depth of the signal as a function of the parameter γ_n at various points of the sample. If at a certain point the value has maximum visibility for some $\gamma_n = \gamma_N$, this means that, according to Eq. (6), the probed point is most closely placed on a plane that has an altitude of Δz_N from the reference mirror, given by

$$\Delta z_N = \gamma_N \lambda f^2 / 2. \quad (7)$$

By this procedure we have the necessary information to measure the profile.

If the tested surface is tilted relative to the transverse plane by small angles (θ_x, θ_y) , the ± 1 longitudinal coherence orders cannot detect the elevation difference between the mirrors because maximum visibility no longer appears on the longitudinal axis $(0, 0, \Delta z)$. This is because, according to the relation $(\Delta x, \Delta y) = [f \tan(2\theta_x), f \tan(2\theta_y)]$, $(\Delta x, \Delta y)$ are different than zero. To find the tilt angle and the elevation, one has to transversely shift the FZP by gradually changing the parameters (ξ_k, η_l) until maximum visibility is obtained on the detector. Assuming this maximum visibility happens for certain value sets of $(\xi_k, \eta_l, \gamma_N)$ then, according to Eq. (6), the tilt angles are

$$\theta_x = \frac{1}{2} \arctan\left(\frac{\Delta x}{f}\right) \\ = \frac{1}{2} \arctan\left[\frac{\gamma_N \lambda f^2 \xi_k}{f(L+2\Delta z_N)}\right] \\ = \frac{1}{2} \arctan\left[\frac{2\Delta z_N \xi_k}{f(L+2\Delta z_N)}\right], \quad (8)$$

$$\theta_y = \frac{1}{2} \arctan\left(\frac{\Delta y}{f}\right) \\ = \frac{1}{2} \arctan\left[\frac{\gamma_N \lambda f^2 \eta_l}{f(L+2\Delta z_N)}\right] \\ = \frac{1}{2} \arctan\left[\frac{2\Delta z_N \eta_l}{f(L+2\Delta z_N)}\right]. \quad (9)$$

The depth resolution of the system is determined by the width of the first order of $\mu(\Delta x, \Delta y, \Delta z)$. According to relation (6), the smallest distinguishable altitude difference is

$$\Delta z_{\min} = 2\lambda f^2 / R^2. \quad (10)$$

The transverse resolution is conventionally determined by the imaging lens L_2 . The angular resolution is approximately the ratio between the transverse width of the first coherence order and its distance Δz_N from the origin:

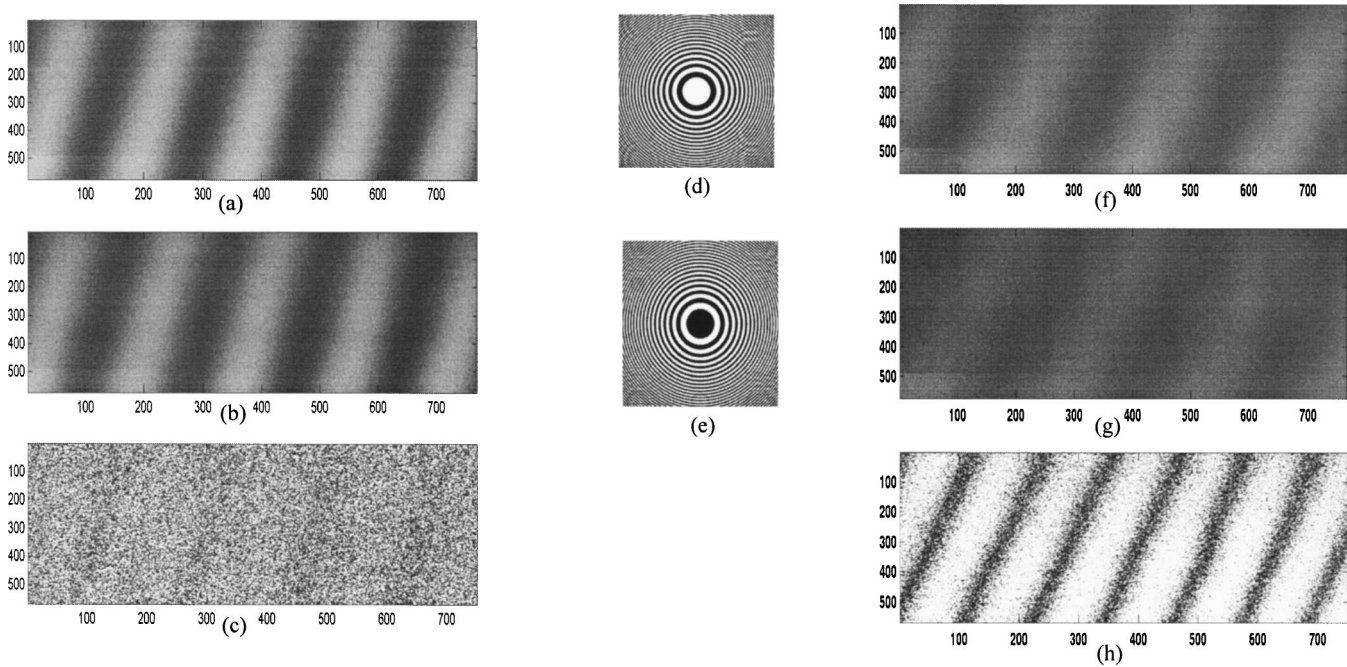


Fig. 2 (a) Interference pattern in the regime of the zero coherence order for $\beta=0$; (b) same as (a) for $\beta=\pi$, (c) subtraction result between the fringe images of (a) and (b); (d) FZP with parameters: $\gamma_n = 7 \text{ cm}^{-2}$, $\beta=0$; (e) FZP with parameters: $\gamma_n = 7 \text{ cm}^{-2}$, $\beta=\pi$; (f) interference pattern in the regime of the first coherence order created by the FZP of (d) with $\beta=0$; (g) same as (h) for FZP of (e) with $\beta=\pi$; and (h) subtraction results between the fringe images of (f) and (g).

$$\Delta \theta_{\min} = \frac{1.22\lambda f^2}{(L + 2\Delta z_{\text{AVERAGE}})R\Delta z_N}. \quad (11)$$

Note that for not too rough surfaces, the system can become almost insensitive to the tilt, if the distance L is chosen to be $L = -2\Delta z_{\text{AVERAGE}}$. In this case, we can measure the surface profile by changing only two parameters γ_n and β_m without considering the small tilts of the tested surface.

3 Experimental Results

Experiments have been conducted to demonstrate the validity of the theory described previously. A schematic illustration of the experimental system is shown in Fig. 1 and has been explained in a previous section. The focal lengths of lenses L_1 and L_2 were $f=250 \text{ mm}$ and $f_2=200 \text{ mm}$, respectively, and the interferometer was illuminated by an He-Ne laser with a wavelength of $\lambda = 0.6328 \mu\text{m}$.

In the first experiment a single mirror was used as the sample. We demonstrate that changes of the variable β_m move only fringes of the first order on the (x,y,L) plane as indicated by Eq. (6). Pictures of the fringes of the zero and first orders with two values of $\beta_{1,2}$: 0 and π were recorded. Changing β_m by π is achieved by contrast inversion of the FZP, as shown in Figs. 2(d) and 2(e). As a result, the fringes of the first order are the only ones to be shifted by a half period, as shown in Figs. 2(f) and 2(g). This π shift can be easily observed by subtracting the last two fringe patterns, as shown in Fig. 2(h). On the other hand, changing β_m does not move the fringes caused by the zero coherence order, as shown in Figs. 2(a) and 2(b), and in their subtraction image, shown in Fig. 2(c). This phenomenon qualitatively

demonstrates that the degree of coherence obeys Eqs. (3) and (6), and help us to find the maximum visibility caused by the first coherence order, as shown next.

We used the subtraction technique of two fringe patterns taken under two opposite contrast FZPs (i.e., with $\beta_1=0$ and $\beta_2=\pi$, as described in Fig. 2) to qualitatively demonstrate that the first order can be moved along the Δz axis and probe surfaces with different elevations. The subtraction technique gives better fringe contrast, and better distinction from the fringes of the zero coherence order, than using a single FZP, as demonstrated by Fig. 2. An experiment was done with three side-by-side mirrors with different elevations relative to the transverse plane. The radius of the incoherent source was 1.8 cm. So according to Eq. (10), the smallest distinguishable altitude difference was $\Delta z_{\min} \approx 0.24 \text{ mm}$. The SLM used here has 1024×768 pixels. Five different values of γ_n were used in the experiment: $\gamma_{1,\dots,5} = 4, 6.64, 9.4, 10.5, 13 \text{ cm}^{-2}$. According to Eq. (7) the five values of γ_n reveal five different altitudes $\Delta z_{1,\dots,5} = 0.79, 1.3, 1.86, 2.08, 2.6 \text{ mm}$. As shown in Fig. 3(c), when γ_n reveals an altitude of a certain mirror, maximum fringe visibility is seen on the corresponding mirror. The states of the degree of coherence for each FZP [shown in Fig. 3(a)] in relation to the altitudes of the three mirrors are shown in Fig. 3(b). In three cases of the FZP, the first, third, and fifth, the distance between the zero and the first coherence orders is equal to twice the distance between the reference mirror and the corresponding (out of the three) mirror.

The next experiment is devoted to the surface profilometry by using the technique of changing the phase parameter β_m . Two mirror steps with different depths between

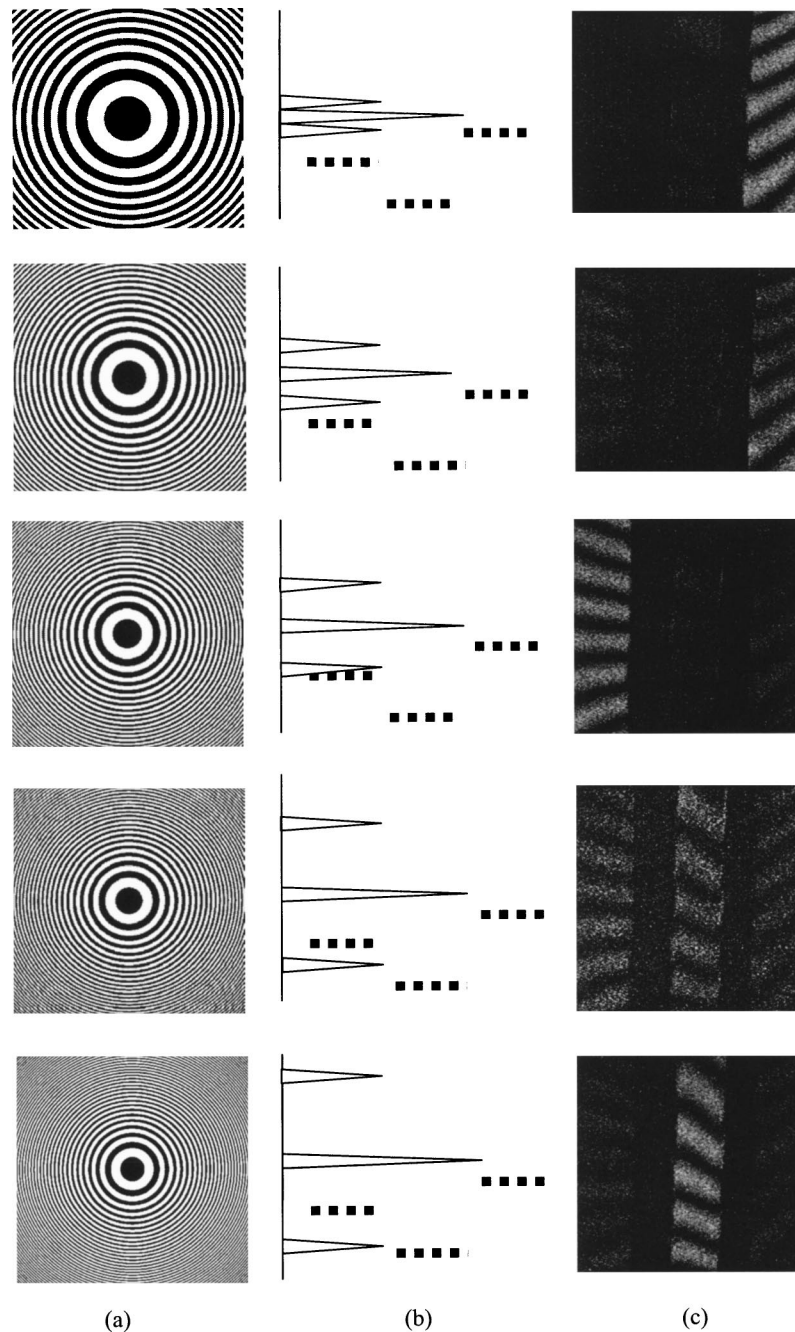


Fig. 3 (a) Set of zone plates with different values of γ_n and $\beta_m = \pi$. (b) Scheme of the complex degree of coherence in relation to three mirrors positions. (c) Absolute value of the subtraction between two fringe images taken with β_m equal to 0 and π .

the mirrors were tested. For each value of γ_n we changed the value of β_m in the range of $[0, 10\pi]$ with a step of $\pi/4$. Therefore, for each value of γ_n we had periodic signals of 41 pixels in length. The experiment was carried out at 350 spatial points along one horizontal line. The measured intensity versus β_m for three values of γ_n at the same position on the mirrors is shown in Fig. 4. For each measurement point on the mirrors, the signal with the maximum modulation depth determines the altitude of the point according to the value of γ_n at that point and Eq. (7).

The two-dimensional profile along a line crossing the two different mirror steps at $y = 200$ pixels, for two different mirror steps, is shown in Figs. 5(a) and 5(b). Altitudes of the mirrors were measured with an uncertainty range of $100 \mu\text{m}$ to each side, which is in the range of inherent uncertainty of $240 \mu\text{m}$ calculated from Eq. (10). Between the two experiments, the right-hand mirror was moved forward a distance of $300 \mu\text{m}$. According to these experiments the altitude gap between the mirrors is estimated to be $150 \mu\text{m}$ in Fig. 5(a) and $500 \mu\text{m}$ in Fig. 5(b). Note that Fig. 5

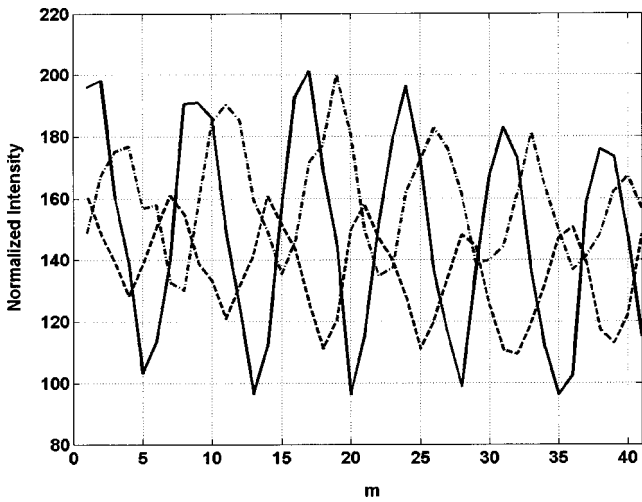


Fig. 4 Normalized intensity on the CCD as a function of m for the point $(x,y)=(100,200)$ pixels on the left mirror. The intensities were measured for the values of $\gamma_n=5.5, 7.5,$ and 9.5 cm^{-2} (dash-dot, solid, dashed line, respectively).

demonstrates a different profile measurement than the experiment shown in Fig. 3. Instead of looking for events of high visibility in the spatial pattern of the interference as in Fig. 3, we look for events of high modulation depth in one-dimensional signals recorded from many scanning points along the surface. Thus by this last method we can measure the altitude of plane segments with a size smaller than the width of a single spatial fringe.

In the last experiment we consider the capability of the system to measure the tilt angles of flat surfaces. The sample mirror was tilted in the (x,z) plane for three different angles: $\theta_x=2.6 \times 10^{-4}, 5.3 \times 10^{-4},$ and 7.9×10^{-4} rad. The FZP was transversely shifted along the x_s axis with step of 8 pixels of the SLM, where for each step an interference pattern was recorded into the computer. In this experiment $\gamma=7.5 \text{ cm}^{-2}$ and according to Eq. (7), $\Delta z = 1.48 \text{ mm}$. A shift of the FZP by one pixel on the SLM is equal to a shift of $40 \mu\text{m}$ of the quasimonochromatic source. Visibility of the interference pattern for the three mentioned angles of the mirror versus the FZP shift is depicted in Fig. 6. As the mirror angle increases, the values of visibility along the plot decreases. The value of the FZP shift increases with the tilt angle to reach the maximum visibility, as expected from Eqs. (8) and (9).

Finally, we verify that the system obeys Eqs. (8) and (9), used here as the main tool to measure a tilt angle of the sample. To study the tolerance of the measurements, we took ten measurements for every mirror tilt angle and calculated the mean and the standard deviation values of the FZP shift. The step of the FZP shift is equal to 8 pixels of the SLM. The solid line of Fig. 7 shows the experimental plot of FZP shift, in which maximum visibility is obtained, versus the tilt angle. These results are compared to the theoretical plot (dash-dot line) calculated by the inverse version of Eq. (8), given by

$$\xi_K = \frac{f(L+2\Delta z)}{2\Delta z} \tan(2\theta_x). \quad (12)$$

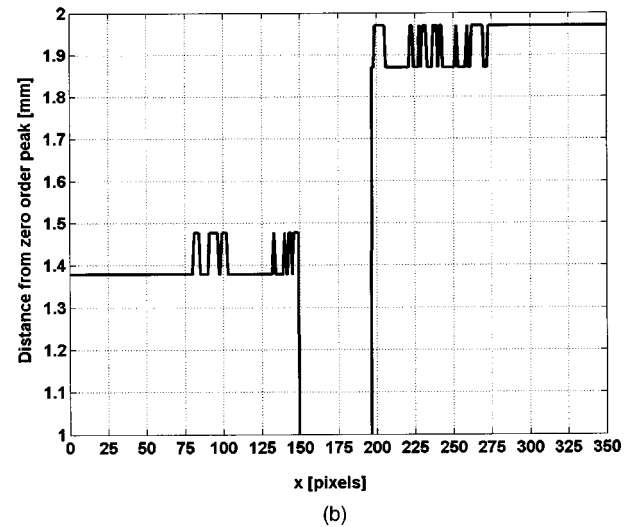
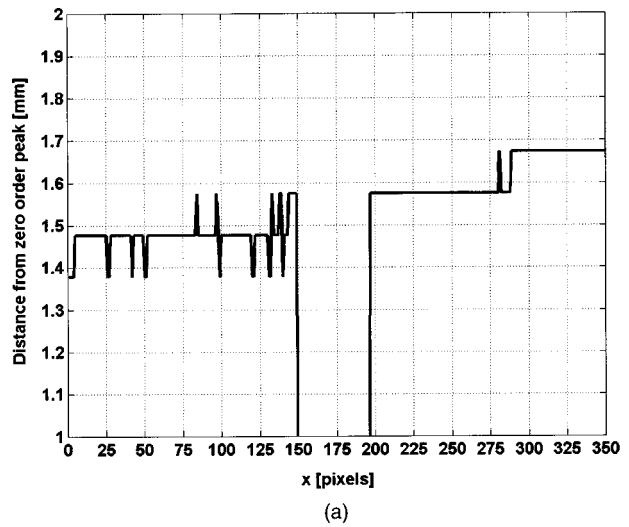


Fig. 5 Cross-section profile of two mirrors along the line $y=200$ pixels. The depth difference between the two mirrors is estimated as (a) $150 \mu\text{m}$ and (b) $500 \mu\text{m}$.

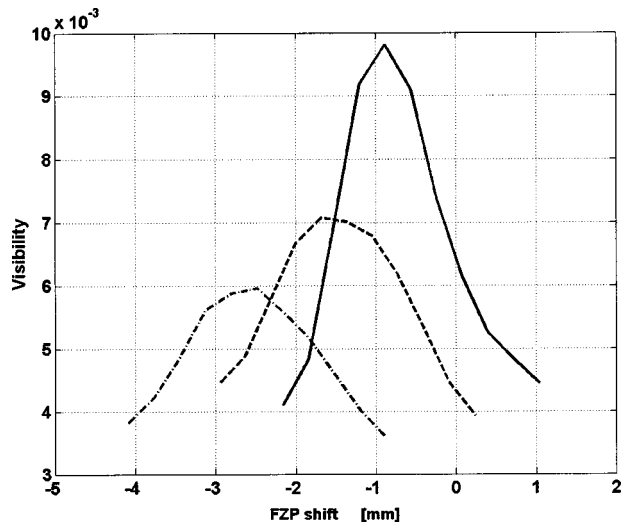


Fig. 6 Visibility of the interference pattern as a function of the FZP shift for different angles of the mirror. The shift step of the FZP on the SLM is equal to 8 pixels.

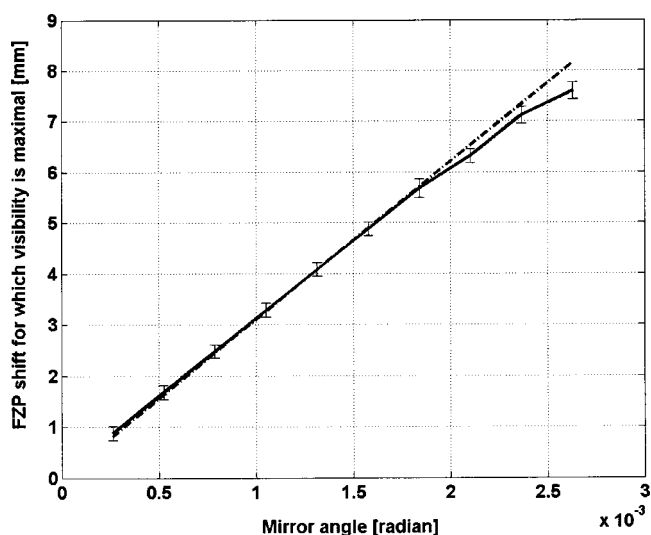


Fig. 7 FZP shift for which the visibility is maximal as a function of the mirror angle. The dashed line is the theoretical plot and the solid line combines the experimental points.

The match between the two plots is good until the angle of 1.6×10^{-3} rad. The theoretical plot was calculated with the following parameters: $f = 250$ mm, $L = 15.4$ mm, and $\Delta z = 1.48$ mm. Note that by forcing the value $L = 0$ (achieved by imaging the back focal plane of lens L_1 into the CCD), the transverse shift of the FZP becomes independent of the elevation difference Δz . Thus, for surfaces with different depths but with the same tilt angle, a single transverse shift of $\xi_k = f \tan(2\theta_x)$ of the FZP will be suitable for measuring all the surfaces.

4 Conclusion

We have demonstrated full control of our proposed spatial coherence radar. The peak of relatively high coherence can desirably move in three axes of the space in which the degree of coherence is defined. The longitudinal movement is used to determine the elevation of the investigated surface, whereas the transverse movement is used for measuring the surface tilt. In addition, we show that the coherence peak's phase angle can be controllably changed. This last parameter enables us to determine the altitude and tilt of small surfaces. The smallest area that can be observed is within the transverse resolution limit of the system.

The main weakness of the present setup, which should be considered in the near future, is the relatively low depth resolution compared to the temporal coherence-based systems. However, the advantageous features of the method are operation without mechanical movement and under quasimonochromatic illumination. The last feature makes the proposed system suitable for measurement in highly dispersive media.

Acknowledgment

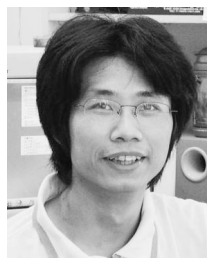
Grant-in-Aid for Scientific Research (No. 13450029) from the Japan Society for the Promotion of Science.

References

1. T. Dresel, G. Hausler, and H. Vezke, "Tree dimensional sensing of rough surfaces by coherence radar," *Appl. Opt.* **31**, 919–925 (1992).
2. B. S. Lee and T. C. Strand, "Profilometry with a coherence scanning microscope," *Appl. Opt.* **29**, 3784–3788 (1990).
3. L. Mandel and E. Wolf, *Optical Coherence and Quantum Optics*, 1st ed., Chap. 4, p. 149, Cambridge University, United Kingdom (1995).
4. J. E. Biegen, "Determination of the phase change on reflection from two-beam interference," *Opt. Lett.* **19**, 1690–1692 (1994).
5. J. Rosen and M. Takeda, "Longitudinal spatial coherence applied for surface profilometry," *Appl. Opt.* **39**, 4107–4111 (2000).
6. W. Wang, H. Kozaki, J. Rosen, and M. Takeda, "Synthesis of longitudinal coherence functions by spatial modulation of an extended light source: a new interpretation and experimental verifications," *Appl. Opt.* **41**, 1962–1971 (2002).
7. J. Rosen and A. Yariv, "General theorem of spatial coherence: application to three dimensional imaging," *J. Opt. Soc. Am. A* **13**, 2091–2095 (1996).



Mark Gokhler received his BA degree in physics from the University of Tashkent in 1990. In 1996 he received an MS degree in applied physics from Hebrew University in Jerusalem. He is currently pursuing his PhD degree in the Department of Electrical and Computer Engineering at Ben-Gurion University of the Negev, Israel. His research interests are optical tomography and statistical optics.



Zhihui Duan received the BS degree with highest honors in mechanical engineering from the University of Science and Technology of China (USTC) in 2000. In 2001 he received the fellowship "Association of International Education, Japan" as an exchange student, and studied at the University of Electro-Communications in Japan. He is currently working towards the MSc degree in mechanical engineering at USTC. His research interests include optical topography, and the

design and fabrication of MEMS.

Joseph Rosen received his DSc in electrical engineering from the Technion-Israel Institute of Technology in 1992. He is currently an associate professor in the Department of Electrical and Computer Engineering, Ben-Gurion University of the Negev. He has coauthored more than 50 scientific papers in refereed journals. His research interests include image processing, diffractive optics, interferometry, pattern recognition, holography, optical tomography, and statistical optics.



Mitsuo Takeda is Professor of Information and Communication Engineering at the University of Electro-Communications (UEC), Tokyo, Japan. He received the BS degree in electrical engineering from UEC in 1969, and the MS and the PhD degrees in applied physics from the University of Tokyo, in 1971 and 1974, respectively. After working for Canon Incorporation, he joined the faculty of UEC in 1977. During 1985 he was a visiting scholar at Stanford University. From 1993 to 1995, he served on the Board of Directors of the Japan Society of Applied Physics, and was a Vice President of the Optical Society of Japan in 1998. He is currently an associate editor of *Optical Review*, and a member of the Editorial Board of *Optics and Lasers in Engineering*. He is a Fellow of SPIE and a member of the International Order of the Knights of Holography.